Microfluid Nanofluid (2011) 11:743–752
DOI 10.1007/s10404-011-0839-9

RESEARCH PAPER

Continuous-flow particle and cell separations in a serpentine microchannel via curvature-induced dielectrophoresis

Junjie Zhu · Robert Cameron Canter · Gyunay Keten · Pallavi Vedantam · Tzuen-Rong J. Tzeng · Xiangchun Xuan

Received: 10 May 2011 / Accepted: 14 June 2011 / Published online: 7 July 2011

Abstract Particle and cell separations are critical to chemical and biomedical analyses. This study demonstrates a continuous-flow electrokinetic separation of particles and cells in a serpentine microchannel through curvature-induced dielectrophoresis. The separation arises from the particle size-dependent cross-stream dielectrophoretic deflection that is generated by the inherent electric field gradients within channel turns. Through the use of a sheath flow to focus the particle mixture, we implement a continuous separation of 1 and 5 μm polystyrene particles in a serpentine microchannel under a 15 kV/m DC electric field. The effects of the applied DC voltages and the serpentine length on the separation performance are examined. The same channel is also demonstrated to separate yeast cells (range in diameter between 4 and 8 μm) from 3 μm particles under an electric field as low as 10 kV/m. The observed focusing and separation processes for particles and cells in the serpentine microchannel are reasonably predicted by a numerical model.

Keywords Microfluidics · Electrokinetics · Particle separation · Dielectrophoresis · Curvature · Serpentine microchannel

J. Zhu · R. C. Canter · G. Keten · X. Xuan (✉)
Department of Mechanical Engineering, Clemson University, Clemson, SC 29634-0921, USA
e-mail: xcxuan@clemson.edu

P. Vedantam · T.-R. J. Tzeng
Department of Biological Sciences, Clemson University, Clemson, SC 29634-0314, USA

1 Introduction

Particle and cell separations are critical to chemical and biomedical analyses. Various techniques have been developed to separate particles in microfluidic devices (Pamme 2007; Kersaudy-Kerhoas et al. 2008; Tsutsui and Ho 2009; Lenshof and Laurell 2010; Gossett et al. 2010). Continuous-flow separations can operate in either an active or a passive mode. For the former, an external gravitational (Huh et al. 2007), electrical (Zhang and Manz 2003), optical (Kim et al. 2008), magnetic (Pamme 2006; Zhu et al. 2010b), or acoustic (Shi et al. 2009) force acts on the aligned particle mixture at an angle to the flow direction and deflects particles to different flow paths. To make this happen, however, additional force(s) is(are) usually required to actuate the particulate solution and align the suspended particles. Passive continuous-flow separations utilize the channel topology-induced force to manipulate particles to differential equilibrium positions during their travel. This type of techniques cover hydrodynamic filtration- (Yamada and Seki 2005), hydrophoresis- (Choi and Park 2009), and inertia-based (Wu et al. 2009; Kuntaegowdanahalli et al. 2009; Di Carlo 2009) continuous separations. In addition, pinched flow fractionation (Takagi et al. 2005) and separation through deterministic lateral displacement (Davis et al. 2006) may also be viewed as passive methods.

Dielectrophoresis (DEP) is another powerful tool for particle manipulation (Morgan and Green 2002; Lapizco-Encinas and Rito-Palmomares 2007; Kang and Li 2009; Hawkins et al. 2009; Xuan et al. 2010), and has been realized mainly by using electrode- (Gascoyne and Vykoukal 2002; Hughes 2002; Pethig 2010) and insulator-based (Chou and Zenhausern 2003; Cummings 2003; Srivastava et al. 2010) approaches. Electrode-based

dielectrophoresis (eDEP) separators employ high-frequency AC electric voltages imposed upon in-channel microelectrodes to create electric field gradients (Choi and Park 2005; Kralj et al. 2006; Chen and Du 2007; Demierre et al. 2007; Kim et al. 2007; Vahey and Voldman 2008; Han and Frazier 2008; Wang et al. 2009; Khoshmanesh et al. 2009; Zhang et al. 2009; Lewpiriyawong et al. 2010; Khoshmanesh et al. 2010). Such active particle separations arise from the dependence of DEP on AC field frequency and particle properties. This type of method, however, suffers from the fabrication complexity and surface fouling of microelectrodes. While contactless eDEP removes these issues (Shafiee et al. 2009, 2010) by isolating electrodes physically from the particle solution, the use of typically 1 MHz-level AC field frequency of the state-of-the-art amplifiers leads to significantly limited applications. Moreover, a pressure-driven pumping of the particle solution is necessary in all eDEP devices to allow for continuous operation.

Insulator-based dielectrophoresis (iDEP) eliminates the difficulties accompanying eDEP by using insulating hurdles, posts, and ridges etc. to locally squeeze the electric current passage and generate electric field gradients (Lapizco-Encinas et al. 2004; Barrett et al. 2005; Kang et al. 2006b; Pysher and Hayes 2007; Hawkins et al. 2007; Sabounchi et al. 2008; Lewpiriyawong et al. 2008; Kang et al. 2008; Jen and Chen 2009; Zhu and Xuan 2009a; Chen and Du 2010; Baylon-Cardiel et al. 2010; Srivastava et al. 2011). Both DC and AC (of any frequency) electric voltages can be applied to the electrodes positioned in end-channel reservoirs, actuating the particle solution by DC electrokinetics and controlling particle transport by DC and AC DEP. Therefore, iDEP separators work in a passive mode. However, the in-channel obstacles may cause adverse effects on the particles (especially to vulnerable cells) to be separated (Voldman 2006) and the device as well because of the potential Joule heating (Hawkins and Kirby 2010; Sridharan et al. 2011) and particle-clogging issues (Simmons et al. 2006).

Recently, our group developed a new passive method to separate particles in serpentine or spiral microchannels using curvature-induced dielectrophoresis (Zhu et al. 2009; Zhu and Xuan 2009b; Church et al. 2009). This method exploits the inherent electric field gradients formed within microchannel turns to manipulate particles by DEP (Ai et al. 2010). Hence, the above-mentioned negative effects caused by the micro-obstacles in iDEP devices are mitigated. It was found that large particles migrate toward the center plane of a serpentine microchannel because of negative DEP, while small particles line the channel sidewalls because of positive DEP (Church et al. 2010b). This separation requires the electric conductivity of the suspending medium be in between those of the two types of particles. Using a very high DC-biased AC electric field, we also demonstrated that large particles bounce between the two sidewalls in a serpentine microchannel due to the extremely strong negative DEP, while small particles migrate to the center (Church et al. 2011). This method is not suitable for handling biological cells as they can be easily damaged or even lysed in large electric fields (Voldman 2006; Church et al. 2010a). In addition, we implemented a continuous particle separation in a spiral microchannel via curvature-induced DEP, where particles are focused to a stream flowing near the outer wall of the first spiral and then deflected to size-dependent flow paths in the second spiral (Zhu et al. 2010a). This method needs to use a very long channel to produce sufficient DEP at mild electric fields (20–30 kV/m).

In this study, we demonstrate a continuous separation of particles and cells by size in a modified serpentine microchannel. Unlike the two designs we have developed recently (Church et al. 2010b, 2011), in this study, a sheath flow is used to focus the particle mixture which is then subjected to curvature-induced DEP for a size-dependent separation in the serpentine section. With such a modification, particles and cells can be separated in a shortened serpentine channel at a reduced DC electric field. These advantages will facilitate the integration of the developed continuous sorter into lab-on-a-chip devices for applications with real biological samples. We also develop a numerical model to simulate the particle and cell separation processes and to optimize the channel structure and working parameters.

2 Experiment

2.1 Microchannel fabrication

The serpentine microchannel was fabricated with poly(dimethylsiloxane) (PDMS) using the standard soft lithography technique. The detailed procedure is given elsewhere (Zhu and Xuan 2009a). Figure 1 shows the picture of the device used in the experiment. The channel has a 1-cm-long serpentine section (composed of totally 33 periods) in the middle with two 3.5-mm-long straight sections at each of its two ends. All sections are 50 μm wide and 25 μm deep. The four reservoirs are labeled with A–D in Fig. 1 to facilitate later descriptions.

2.2 Particle and cell mixtures preparation

Green fluorescent polystyrene particles of 1 μm (Bangs Laboratories, Fisher, IN) and 5 μm (Duke Scientific, Waltham, MA) in diameter were mixed at 1:50 volume ratio and re-suspended in 1 mM phosphate buffer with a

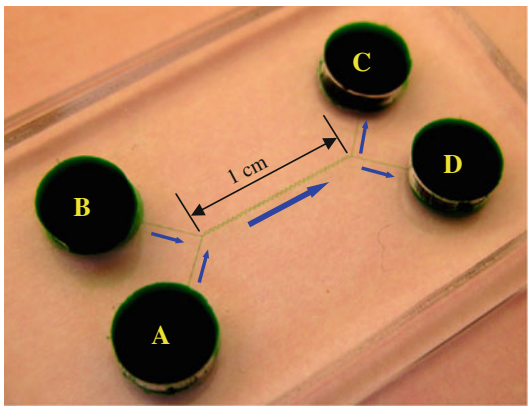

Fig. 1 Picture of the serpentine microchannel (filled with food dye for clarity) used in the experiment. The block *arrows* indicate the flow directions during the separation process. The four reservoirs are highlighted with letters *A–D*

final concentration of 10^7–10^8 particles per ml. ATCC4098 yeast cells (*Saccharomyces cerevisiae*) were cultured using the same protocol as described in Church et al. (2009). Their diameters range between 4 and 8 μm with an average of 6 μm. Yeast cells were mixed with 3-μm-diameter polystyrene particles (Sigma Aldrich, St Louis, MO) and then re-suspended in 1 mM phosphate buffer at about 10^7–10^8 particles or cells per ml. Tween 20 (Fisher Scientific, Waltham, MA) was added to both the particle and cell mixtures at 0.1% v/v to suppress the aggregation of particles and cells and their adhesion to channel walls.

2.3 Particle manipulation and visualization

The continuous separation of particles and cells in the serpentine microchannel was achieved through curvature-induced DEP by the application of DC electric fields. A DC power supply (Glassman High Voltage) in conjunction with a custom-made voltage controller was employed to supply electric voltages to the electrodes placed in reservoirs. Reservoir A (see Fig. 1) was injected with the particle or cell mixture, and the remaining reservoirs (i.e., B–D in Fig. 1) were all filled with 1 mM buffer. Before each test, pressure-driven particle or cell motion was eliminated by carefully balancing the liquid heights in the four reservoirs.

3 Theory

3.1 Working mechanism

Figure 2 shows the electric field lines and contour (quantified by the background color, the darker, the higher) in the entrance region of the channel's serpentine section (see Fig. 1). It is important to note that electric field lines are similar to fluid streamlines in pure electrokinetic flows (Santiago 2001). As indicated by the squeezed dark streamlines from reservoir A, the particle (or cell) mixture is first focused by the sheath fluid (see the light streamlines from reservoir B) to a stream flowing near the channel wall. Then, in the serpentine section of the microchannel, the focused particles experience DEP in every corner because of the local electric field gradients (Zhu et al. 2009; Ai et al. 2010). As polymer particles and biological cells appear to be poorly conducting in DC electric fields (Ermolina and Morgan 2005; Pethig and Markx 1997), they are often less polarizable than the suspending fluid yielding negative DEP. The resulting dielectrophoretic velocity, $\mathbf{U}_{DEP}$, thus deflects the focused particles away from the inner corner of a turn as depicted in Fig. 2.

Using the effective dipole moment method, we can obtain the following formulae for $\mathbf{U}_{DEP}$ in DC electric fields (Kirby 2010):

$$\mathbf{U}_{DEP} = \mu_{DEP}(\mathbf{E} \cdot \nabla \mathbf{E}) \tag{1}$$

$$\mu_{DEP} = \frac{\varepsilon_f d^2}{6\mu_f} \frac{\sigma_p - \sigma_f}{\sigma_p + 2\sigma_f} \tag{2}$$

where μ_{DEP} is the dielectrophoretic mobility of particles, $\mathbf{E}$ is the local electric field, ε_f is the permittivity of the fluid, d is the particle diameter, μ_f is the fluid viscosity, σ_p is the electric conductivity of particles or cells, and σ_f is the electric conductivity of the fluid. The cross-stream dielectrophoretic velocity, $\mathbf{U}_{DEP}$, competes with the streamwise electrokinetic velocity, $\mathbf{U}_{EK}$, the result of which determines

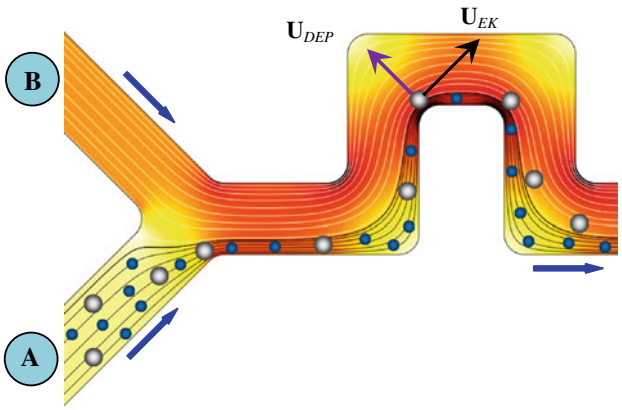

Fig. 2 Illustration of sheath-flow focusing and dielectrophoretic separation of particles (represented by *filled circles* of different diameters) in a serpentine microchannel. The *dark* and *light lines* represent the streamlines starting from reservoir *A* (filled with the particle or cell mixture) and reservoir *B* (filled with the sheath fluid), respectively. The background displays the electric field contour (the *darker*, the higher) in the absence of particles. The block *arrows* indicate the flow directions. See Fig. 1 for the configuration of the channel and reservoirs

the transverse *deflection* of particles. If two types of particles have a similar or comparable $\mathbf{U}_{EK}$, then larger particles should be deflected farther than smaller ones (see the illustration in Fig. 2) because of the dependence of $\mathbf{U}_{DEP}$ on the particle diameter squared. As a result, the sheath-focused particle mixture can be divided into two sub-streams at the exit of the serpentine section, leading to a continuous size-based sorting of particles into the downstream reservoirs C (to collect larger particles or cells) and D (to collect smaller particles or cells).

3.2 Numerical modeling

We developed a 2D numerical model to simulate the electric field-mediated transport and manipulation of particles and cells in the serpentine microchannel. This model is revised from that developed by Kang et al. (2006a), and has been validated by several experiments performed by our group (Zhu and Xuan 2009a, b; Zhu et al. 2009; Church et al. 2009, 2010a, b, 2011). This model neglects the perturbations of a particle (or cell) to the flow and electric fields, and employs a correction factor, c, to account for the effects of the particle size (and others, such as particle–particle interactions and wall-induced retardation, etc.) on the dielectrophoretic velocity. Hence, the velocity of the particle is written as

$$\mathbf{U}_p = \mu_{EK}\mathbf{E} + c\mu_{DEP}(\mathbf{E}\cdot\nabla\mathbf{E}). \quad (3)$$

where μ_{EK} denotes the electrokinetic mobility which is a combination of electro-osmotic and electrophoretic mobilities. It should be noted that we have neglected the particle velocity due to pressure-driven flow, inertia, and Brownian motion in Eq. 3. The velocity, $\mathbf{U}_p$, is used as an input of the particle-tracing function in COMSOL (Burlington, MA) to compute the particle trajectory. All the particles are assumed massless and uniformly distributed when entering into the channel from the injection reservoir A.

The simulation was carried out in COMSOL. The computational domain comprises the entire microchannel in the horizontal plane. The electric field, $\mathbf{E} = -\nabla\phi$, is obtained by solving the Laplace equation $\nabla^2\phi = 0$ in COMSOL. The boundary conditions include the electric voltages imposed to the four reservoirs and the insulating condition on all the channel walls. The electrokinetic mobility, μ_{EK}, was determined by tracking the motions of individual particles or cells in a straight channel where DEP is negligible. The dielectrophoretic mobility, μ_{DEP}, was calculated from Eq. 2 using the values of the typical dynamic viscosity, $\mu = 1.0 \times 10^{-3}$ kg/(m s) and permittivity $\varepsilon_f = 6.9 \times 10^{-10}$ C/(v m) for pure water at 20°C. The electric conductivity of polystyrene particles with a diameter d was determined using $\sigma_p = 4K_s/d$ with $K_s = 1$ nS being the surface conductance recommended by Ermolina and Morgan (2005). The electric conductivity of yeast cells is dictated by the membrane conductivity in DC electric fields with a value on the order of 1 nS/cm (Hoettges et al. 2008). The electric conductivity of 1 mM phosphate buffer measured 210 μS/cm. The correction factor, c, was determined by fitting the predicted particle or cell trajectories to the experimentally observed pathlines.

4 Results and discussions

4.1 Separation of 1 and 5 μm polystyrene particles

Figure 3 demonstrates a continuous separation of 1 and 5 μm polystyrene particles in the serpentine microchannel via the curvature-induced DEP. The DC voltages imposed to reservoirs A–D (see Fig. 1) are 270, 300, 0 V (i.e., grounded), and 10 V, respectively. The resulting electric field in the serpentine section of the channel is 15 kV/m on average as predicted from the numerical modeling. The measured values of the electrokinetic mobility are approximately the same for the two types of particles, which is 3.5×10^{-8} (m^2/V s). This corresponds to an average particle speed of around 500 μm/s in the serpentine section during the separation process. Therefore, 5 μm particles should obtain a larger dielectrophoretic *deflection* than 1 μm particles in the serpentine section. As seen from the snapshot (a1) and superimposed (a2) images of Fig. 3, both sizes of particles are forced by the sheath fluid to flow near the lower sidewall at the entrance of the serpentine section. The width of the focused particle stream in Fig. 3a2 is a little larger than the diameter of 5 μm particles, implying that 1 μm particles are actually not aligned before entering into the serpentine section. This makes the demonstrated particle separation distinct from the so-called pinched flow fractionation (Yamada et al. 2004; Takagi et al. 2005; Kawamata et al. 2008), where the particles to be separated must all be pushed against one sidewall to allow for the subsequent size-based separation in an expansion channel.

As the focused stream of the particle mixture flows through the serpentine section of the channel, 5 μm particles are gradually displaced out of the stream toward the channel centerline by DEP, while 1 μm particles still remain in the stream because of their much weaker dielectrophoretic response. This is evident from the snapshot (a2) and superimposed (b2) images at the exit of the serpentine section in Fig. 3. As compared with the images at the entrance, it is obvious that 5 μm particles are deflected to the channel centerline and laterally separated from 1 μm particles, the stream of which also becomes wider because of their weak DEP. As a result, 5 and 1 μm

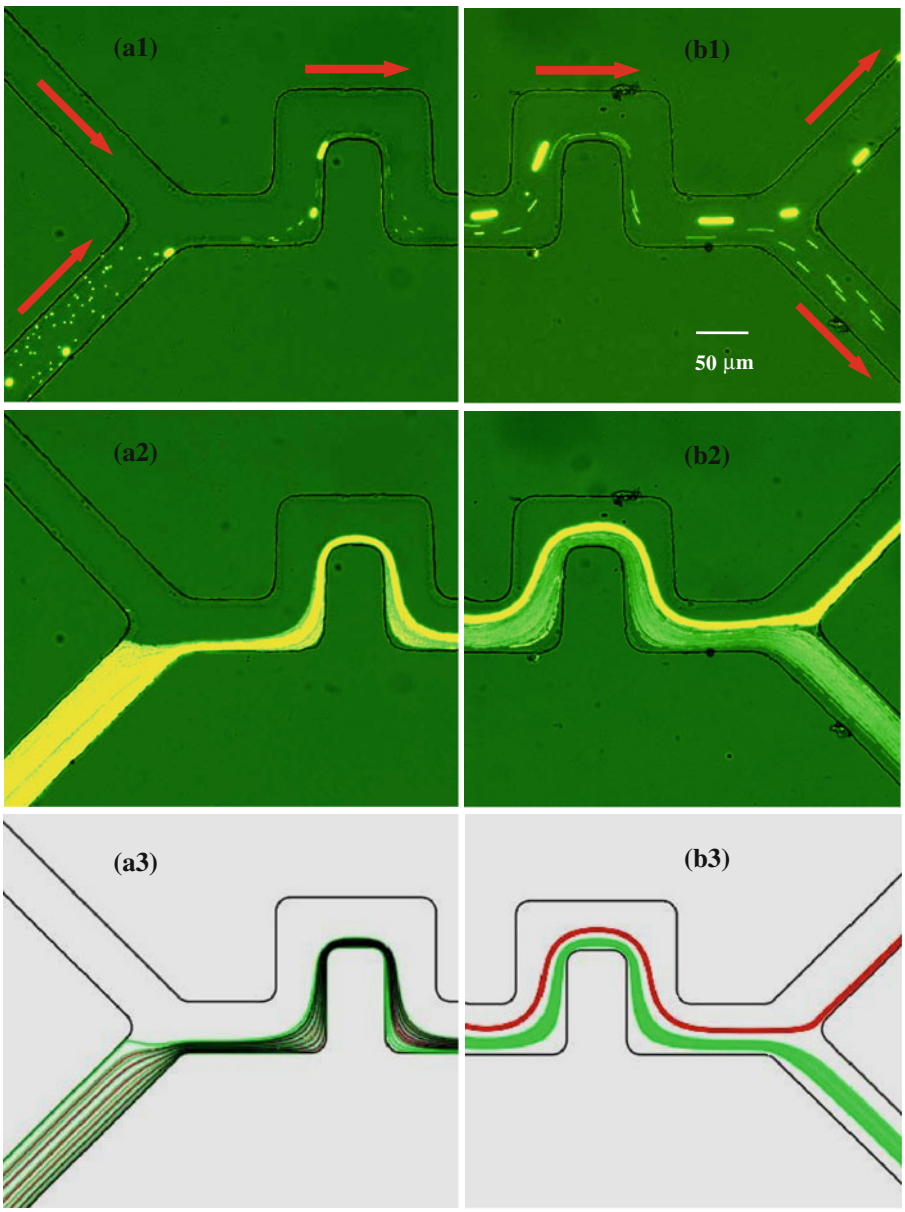

Fig. 3 Continuous separation of 1 and 5 μm polystyrene particles in a serpentine microchannel via the curvature-induced DEP: the *left* column displays the snapshot image (**a1**), superimposed image (**a2**), and numerical prediction (**a3**) of sheath-flow particle focusing at the entrance of the serpentine section; the *right* column displays the snapshot image (**b1**), superimposed image (**b2**), and numerical prediction (**b3**) of dielectrophoretic particle separation at the exit of the serpentine section. It is noted that a longer exposure time was used for the images in the *right* column such that the particles therein appear larger (more accurately, longer) than those in the *left* column. The block *arrows* in the *top-row* images indicate the flow directions

particles are collected into reservoirs C and D, respectively, through an uneven split of the flow following the serpentine section (a slightly larger flow moves to reservoir C due to the 10 V voltage difference between reservoirs C and D). The particle throughput is about 800 particles per minute as estimated from the video at the exit of the channel's serpentine section. It can be enhanced by the use of a higher particle concentration and/or a deeper channel as the curvature-induced DEP does not depend on the channel depth (Zhu et al. 2009). It can also be increased using a wider serpentine channel if Joule heating is not of a significant concern (Xuan 2008).

The numerical predictions of the particle trajectories at the entrance (a3) and exit (b3) of the channel's serpentine section are also displayed in Fig. 3. The exact experimental conditions were used in the modeling. The correction factor, c, for dielectrophoretic velocity was set to 1 and 0.6 for 1 and 5 μm particles, respectively, both of which are consistent with our previous studies (Zhu et al. 2009; Zhu and Xuan 2009a, b; Church et al. 2010b, 2011). It is seen that the model captures the observed focusing and separation behaviors of both types of particles with reasonable agreements. However, the width of the 1 μm particle stream is apparently wider in the experiment than in the simulation. This discrepancy may be due to the neglect of particle diffusion in our numerical model. We estimate that the lateral diffusion of 1 μm particles is $\sqrt{Dt} = 3.8\,\mu\text{m}$ on each side of the stream, where $D = 4.4 \times 10^{-13}$ m^2/s is the particle diffusivity, and $t \approx 32$ s is the travel time. The resultant particle stream width is nearly twice that shown in

Fig. 3b3, and hence should agree better with the experimental image in Fig. 3b2.

4.1.1 *Effects of applied DC voltages*

The numerical model was employed to study how the applied DC voltages in the four reservoirs affect the particle separation in the serpentine microchannel. Three different scenarios are observed as shown in Fig. 4. In the first scenario, the applied voltage drop across the serpentine section is small (hence, the local electric field is low), such that the induced DEP is insufficient to push 5 μm particles out of the sheath-focused mixture stream. As a consequence, 5 and 1 μm particles both flow into reservoir D with no separation at all. This situation is demonstrated in Fig. 4a, where the DC voltages applied to reservoirs A–D are 135, 150, 0, and 5 V, respectively. The second scenario in Fig. 4b is identical to the demonstrated particle separation in Fig. 3, where the DC voltage in each reservoir is twice that in Fig. 4a. In the third scenario, part of the 1 μm particles are also directed to reservoir D along with 5 μm particles because of either a strong DEP for even 1 μm particles in the serpentine section at a very high electric field or an improper split of the flow into reservoirs C and D. This latter circumstance is illustrated in Fig. 4c, where the DC voltages are 270, 300, 0, and 30 V for reservoirs A–D, respectively.

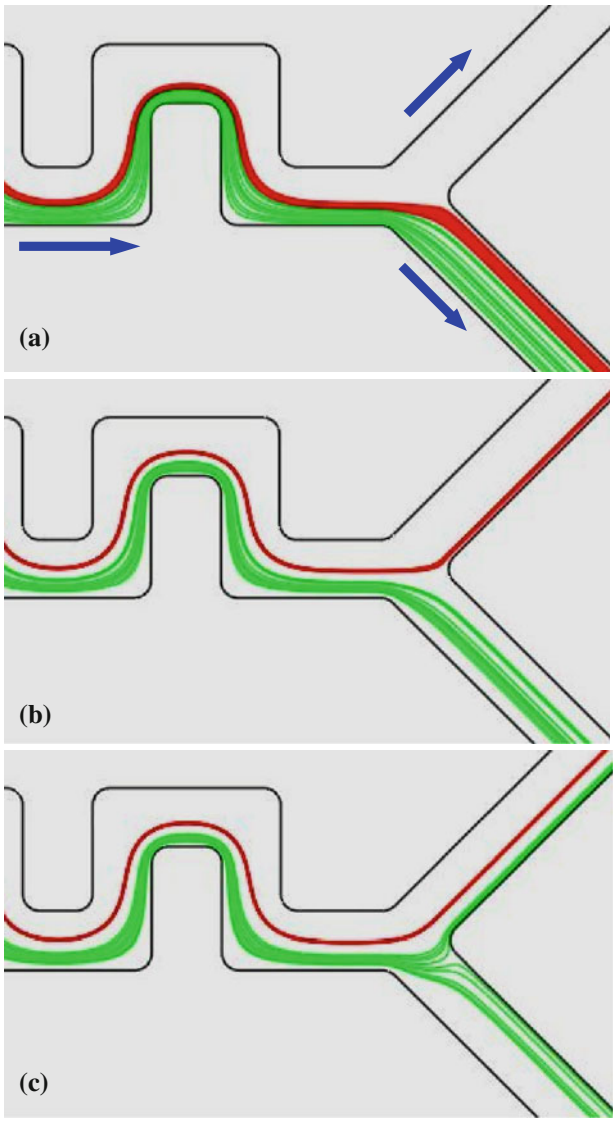

Fig. 4 Numerical study of the voltage effects on the separation of 1 μm (*lower lines*) and 5 μm (*upper lines*) polystyrene particles at the exit of the channel's serpentine section. The DC voltages applied to reservoirs A–D (refer to Fig. 1), respectively, are **a** 135/150/0/5, **b** 270/300/0/10, and **c** 270/300/0/30. All the values are in the unit of volt. The block *arrows* in **a** indicate the flow directions

4.1.2 *Effect of serpentine length*

We also used the numerical model to examine whether the length of the channel's serpentine section (determined by the number of serpentine periods if the length of one period is fixed) can be reduced. For the demonstrated separation of 1 and 5 μm particles in Fig. 3, our model shows that 5 μm particles still mix with 1 μm particles after the first five serpentine periods and, hence, no separation can be achieved at that stage. In the eighth serpentine period, 5 μm particles are displaced from the stream of 1 μm particles by a lateral distance of around 1 μm. This gap increases to 8 μm when both particles have traveled through 16 serpentine periods or nearly one half of the serpentine section (composed of totally 33 periods). It continues to increase up to 11 μm in the 24th period, followed by a nearly unvaried gap in the rest of the periods. Therefore, we estimate that the serpentine section of the current channel can be shortened by at least one quarter while not affecting the separation performance at the same electric field as in Fig. 3. In addition, our model predicts that the current serpentine microchannel is capable of separating 5 μm particles from 3 μm particles, and even 2 μm particles from 3 μm particles, as long as the electric voltages imposed to reservoirs C and D are appropriately adjusted.

4.2 Separation of yeast cells and 3 μm polystyrene particles

Using the current serpentine microchannel, we also separated through curvature-induced DEP *S. cerevisiae* yeasts (with an average diameter of 6 μm) from 3 μm polystyrene particles as demonstrated in Fig. 5. The DC voltages imposed to reservoirs A–D (see Fig. 1) are 180, 200, 0, and 6 V, respectively, producing an average electric field of only 10 kV/m in the serpentine section. As this electric

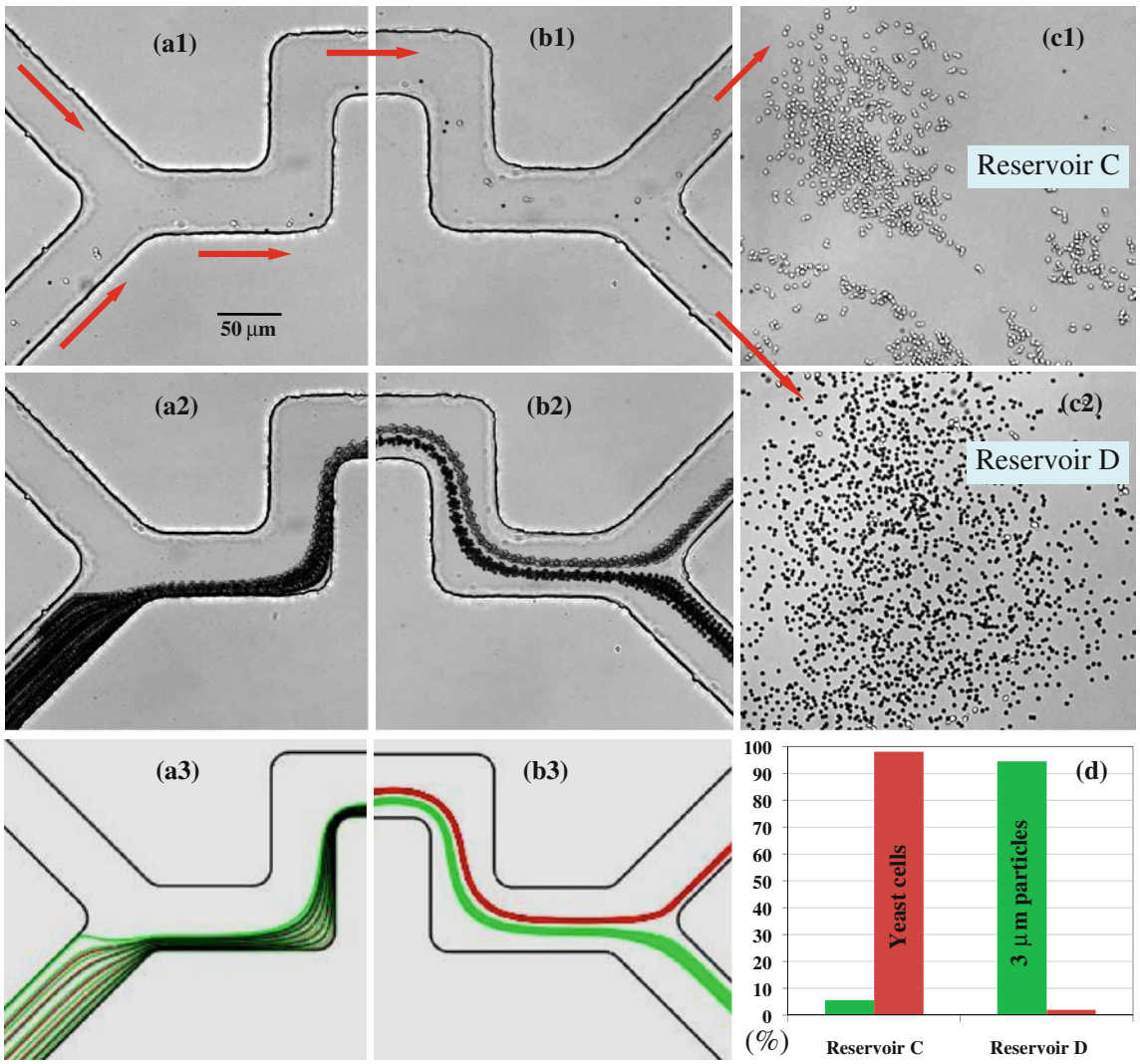

Fig. 5 Continuous separation of yeast cells and 3 μm polystyrene particles in a serpentine microchannel via the curvature-induced DEP: the *left* column displays the snapshot image (**a1**), superimposed image (**a2**), and numerical prediction (**a3**) of sheath-flow particle/cell focusing at the entrance of the serpentine section; the *middle* column displays the snapshot image (**b1**), superimposed image (**b2**), and numerical prediction (**b3**) of dielectrophoretic particle/cell separation at the exit of the serpentine section; the *right* column displays the images of the sorted particles and cells in reservoirs *C* (**c1**) and *D* (**c2**) of the microchannel and the corresponding column charts of particle/cell percentages in each reservoir (**d**). The block arrows indicate the flow directions

field level has been proved safe for even vulnerable mammalian cells (Voldman 2006), we anticipate that the curvature-induced DEP in serpentine microchannels can be used with potential to separate real cell mixtures for biomedical and clinical applications. The measured electrokinetic mobility values are 2.8×10^{-8} and 3.5×10^{-8} (m^2/V s) for the yeast cells and particles, respectively. Therefore, the larger yeast cells should experience a greater dielectrophoretic *deflection* than the smaller particles in the serpentine section. Moreover, as the measured diameter of the yeast cells actually spans from 4 to 8 μm, the size resolution of this dielectrophoretic separation is estimated to be down to 1 μm, consistent with the prediction of our numerical model as noted above.

At the entrance of the serpentine section (Fig. 5a1), the yeast cells and particles are focused to a stream of about 10 μm in width as measured from the superimposed image (Fig. 5a2). At the exit of the serpentine section, both the yeast cells and the particles are displaced out of the initial sheath-focused stream, but they travel along distinct flow paths in the channel center region (see Fig. 5b1, b2). They are subsequently sorted into reservoirs, C and D. The whole focusing and sorting process is reasonably predicted by the numerical model (see Fig. 5a3, b3). In the simulation, we set the correction factor, *c*, to 0.5 and 0.8 for the yeasts and particles, respectively, which are consistent with previous studies (Zhu et al. 2009; Zhu and Xuan 2009a, b; Church et al. 2010b, 2011).

The throughput of this separation is estimated to be about 200 particles or cells per minute, which can be greatly enhanced if a higher particle/cell concentration and a deeper channel are used. After the separation experiment had been continuously run for 15 min without any interruption or adjustment, we took a snapshot image of the particles and cells sorted to reservoirs C and D as seen in Fig. 5c1 and c2, respectively. An image software was then employed to count the number of yeast cells and particles in the image of each reservoir, and the results (over 2000 particles and cells were counted) are shown as a column chart in Fig. 5d. One can see that the percentage of the sorted yeast cells in reservoir C and the sorted particles in reservoir D are both over 90%, indicating a good purity of the demonstrated separation.

5 Conclusions

We have developed a continuous-flow particle separation method in serpentine microchannels through the curvature-induced DEP. As compared to those separations in curved microchannels demonstrated by our group (Zhu et al. 2010a; Church et al. 2010b, 2011), the current method employs a sheath fluid to focus the particle mixture so that the electric field magnitude and the channel length can both be significantly reduced. We have used this method to implement a continuous separation of 1 and 5 μm particles, where the effects of the applied DC voltages and the serpentine length on the separation performance have been examined. We have also used this method to separate yeast cells from 3 μm particles under an electric field of 10 kV/m. Moreover, the experimentally observed focusing and separation processes of particles and cells are predicted with reasonable agreement by a simple numerical model. We envision that the demonstrated particle and cell separation technique in serpentine microchannels through the curvature-induced DEP can potentially be used for biomedical and clinical applications involving real cell mixtures.

Acknowledgments The supports from the NSF under grant CBET-0853873, and from the Clemson University via a start-up package, and from the Creative Inquiry Program are acknowledged (Xuan).

References

Ai Y, Park S, Zhu J, Xuan X, Beskok A, Qian S (2010) DC electrokinetic particle transport in an L-shaped microchannel. Langmuir 26:2937–2944

Barrett LM, Skulan AJ, Singh AK, Cummings EB, Fiechtner GJ (2005) Dielectrophoretic manipulation of particles and cells using insulating ridges in faceted prism microchannels. Anal Chem 77:6798–6804

Baylon-Cardiel JL, Jesus-Perez NM, Chavez-Santoscoy AV, Lapizco-Encinas BH (2010) Controlled microparticle manipulation employing low frequency alternating electric fields in an array of insulators. Lab Chip 10:3235–3242

Chen DF, Du HJ (2007) A dielectrophoretic barrier-based microsystem for separation of microparticles. Microfluid Nanofluid 3:603–610

Chen DF, Du HJ (2010) A microfluidic device for rapid concentration of particles in continuous flow by DC dielectrophoresis. Microfluid Nanofluid 9:281–291

Choi S, Park JK (2005) Microfluidic system for dielectrophoretic separation based on a trapezoidal electrode array. Lab Chip 5:1161–1167

Choi SY, Park JK (2009) Tuneable hydrophoretic separation using elastic deformation of poly(dimethylsiloxane). Lab Chip 9:1962–1965

Chou CF, Zenhausern F (2003) Electrodeless dielectrophoresis for micro total analysis systems. IEEE Eng Med Biol Mag 22:62–67

Church C, Zhu J, Wang G, Tzeng TJ, Xuan X (2009) Electrokinetic focusing and filtration of cells in a serpentine microchannel. Biomicrofluidics 3:044109

Church C, Zhu J, Huang G, Tzeng TJ, Xuan X (2010a) Integrated electrical concentration and lysis of cells in a microfluidic chip. Biomicrofluid 4:044101

Church C, Zhu J, Nieto J, Keten G, Ibarra E, Xuan X (2010b) Continuous particle separation in a serpentine microchannel via negative and positive dielectrophoretic focusing. J Micromech Microeng 20:065011

Church C, Zhu J, Xuan X (2011) Negative dielectrophoresis-based particle separation by size in a serpentine microchannel. Electrophoresis 32:527–531

Cummings EB (2003) Streaming dielectrophoresis for continuous-flow microfluidic devices. IEEE Eng Med Biol Mag 22:75–84

Davis JA, Inglis DW, Morton KJ, Lawrence DA, Huang LR, Chou SY, Sturm JC, Austin RH (2006) Deterministic hydrodynamics: taking blood apart. Proc Natl Acad Sci USA 103:14779–14784

Demierre N, Braschler T, Linderholm P, Seger U, van Lintel H, Renaud P (2007) Characterization and optimization of liquid electrodes for lateral dielectrophoresis. Lab Chip 7:355–365

Di Carlo D (2009) Inertial microfluidics. Lab Chip 9:3038–3046

Ermolina I, Morgan H (2005) The electrokinetics properties of latex particles: comparison of electrophoresis and dielectrophoresis. J Colloid Interface Sci 285:419–428

Gascoyne PRC, Vykoukal J (2002) Particle separation by dielectrophoresis. Electrophoresis 23:1973–1983

Gossett DR, Weaver WM, Mach AJ, Hur SC, Tse HTK, Lee W, Amini H, Di Carlo D (2010) Label-free cell separation and sorting in microfluidic systems. Anal Bioanal Chem 397:3249–3267

Han KH, Frazier AB (2008) Lateral-driven continuous dielectrophoretic microseparators for blood cells suspended in a highly conductive medium. Lab Chip 8:1079–1086

Hawkins BG, Kirby BJ (2010) Electrothermal flow effects in insulating (electrodeless) dielectrophoresis systems. Electrophoresis 31:3622–3633

Hawkins BG, Smith AE, Syed YA, Kirby BJ (2007) Continuous-flow particle separation by 3D insulative dielectrophoresis using coherently shaped, DC-biased, AC electric fields. Anal Chem 79:7291–7300

Hawkins BG, Gleghorn JP, Kirby BJ (2009) Dielectrophoresis for cell and particle manipulations. In: Zahn JD (ed) Methods in bioengineering: biomicrofabrication and biomicrofluidics. Artech Press, Boston, pp 133–181

Hoettges KF, Hubner Y, Broche LM, Ogin GEN, Kassv MP, Hughes A (2008) Dielectrophoresis-activated multiwell plate for label-free high-throughput drug assessment. Anal Chem 80:2063–2068

Hughes MP (2002) Strategies for dielectrophoretic separation in laboratory-on-a-chip systems. Electrophoresis 23:2569–2582
Huh D, Bahng JW, Ling Y, Wei H, Kripfgans OD, Fowlkes JB, Grotberg JB, Takayama S (2007) Gravity-driven microfluidic particle sorting device with hydrodynamic separation amplification. Anal Chem 79:1369–1376
Jen CP, Chen TW (2009) Selective trapping of live and dead mammalian cells using insulator-based dielectrophoresis within open-top microstructures. Biomed Microdev 11:597–607
Kang Y, Li D (2009) Electrokinetic motion of particles and cells in microchannels. Microfluid Nanofluid 6:431–460
Kang K, Xuan X, Kang Y, Li D (2006a) Effects of the DC-dielectrophoretic force on particle trajectories in microchannels. J Appl Phys 99:064702
Kang K, Kang Y, Xuan X, Li D (2006b) Continuous separation of microparticles by size with DC-dielectrophoresis. Electrophoresis 27:694–702
Kang Y, Li D, Kalams SA, Eid JE (2008) DC-Dielectrophoretic separation of biological cells by size. Biomed Microdev 10:243–249
Kawamata T, Yamada M, Yasuda M, Seki M (2008) Continuous and precise particle separation by electroosmotic flow control in microfluidic devices. Electrophoresis 29:1423–1430
Kersaudy-Kerhoas M, Dhariwal R, Desmulliez MP (2008) Recent advances in microparticle continuous separation. IET Nanobiotechnol 2:1–13
Khoshmanesh K, Zhang C, Tovar-Lopez FJ, Nahavandi S, Baratchi S, Kalantar-zadeh K, Mitchel A (2009) Dielectrophoretic manipulation and separation of microparticles using curved microelectrodes. Electrophoresis 30:3707–3717
Khoshmanesh K, Zhang C, Tovar-Lopez FJ, Nahavandi S, Baratchi S, Mitchell A, Kalantar-Zadeh K (2010) Dielectrophoretic-activated cell sorter based on curved microelectrodes. Microfluid Nanofluid 9:411–426
Kim U, Shu CW, Dane KY, Daugherty PS et al (2007) Selection of mammalian cells based on their cell-cycle phase using dielectrophoresis. Proc Natl Acad Sci USA 104:20708–20712
Kim SB, Yoon SY, Sung HJ, Kim SS (2008) Cross-type optical particle separation in a microchannel. Anal Chem 80:2628–2630
Kirby BJ (2010) Micro- and nanoscale fluid mechanics: transport in microfluidic devices. Cambridge University Press, New York
Kralj JG, Lis MTW, Schmidt MA, Jensen KF (2006) Continuous dielectrophoretic size-based particle sorting. Anal Chem 78:5019–5025
Kuntaegowdanahalli SS, Bhagat AAS, Kumar G, Papautsky I (2009) Inertial microfluidics for continuous particle separation in spiral microchannels. Lab Chip 9:2973–2980
Lapizco-Encinas BH, Rito-Palmomares M (2007) Dielectrophoresis for the manipulation of nanoparticles. Electrophoresis 28:4521–4538
Lapizco-Encinas BH, Simmons BA, Cummings EB, Fintschenko Y (2004) Insulator-based dielectrophoresis for the selective concentration and separation of live bacteria in water. Electrophoresis 25:1695–1704
Lenshof A, Laurell T (2010) Continuous separation of cells and particles in microfluidic systems. Chem Soc Rev 39:1203–1217
Lewpiriyawong N, Yang C, Lam YC (2008) Dielectrophoretic manipulation of particles in a modified microfluidic H-filter with multi-insulating blocks. Biomicrofluidics 2:034105
Lewpiriyawong N, Yang C, Lam YC (2010) Continuous sorting and separation of microparticles by size using AC dielectrophoresis in a PDMS microfluidic device with 3-D conducting PDMS composite electrodes. Electrophoresis 31:2622–2631
Morgan H, Green NG (2002) AC electrokinetic: colloids and nanoparticles. Research Studies Press, Hertfordshire
Pamme N (2006) Magnetism and microfluidics. Lab Chip 6:624–638
Pamme N (2007) Continuous flow separations in microfluidic devices. Lab Chip 7:1644–1659
Pethig R (2010) Dielectrophoresis: status of the theory, technology, and applications. Biomicrofluidics 4:022811
Pethig R, Markx GH (1997) Applications of dielectrophoresis in biotechnology. Trends Biotechnol 15:426–432
Pysher MD, Hayes MA (2007) Electrophoretic and dielectrophoretic field gradient technique for separating bioparticles. Anal Chem 79:4552–4557
Sabounchi P, Morales AM, Ponce P, Lee LP, Simmons BA, Davalos RV (2008) Sample concentration and impedance detection on a microfluidic polymer chip. Biomed Microdev 10:661–670
Santiago JG (2001) Electroosmotic flows in microchannels with finite inertial and pressure forces. Anal Chem 73:2353–2365
Shafiee H, Caldwell JL, Sano MB, Davalos RD (2009) Contactless dielectrophoresis: a new technique for cell manipulation. Biomed Microdev 11:997–1006
Shafiee H, Sano MB, Henslee EA, Caldwell JL, Davalos RD (2010) Selective isolation of live/dead cells using contactless dielectrophoresis (cDEP). Lab Chip 10:438–445
Shi JJ, Huang H, Stratton Z, Huang YP, Huang TJ (2009) Continuous particle separation in a microfluidic channel via standing surface acoustic waves (SSAW). Lab Chip 9:3354–3359
Simmons BA, Cummings EB, Davalos RV et al (2006) Separation and concentration of water-borne contaminants utilizing insulator-based dielectrophoresis. SAND2006-0654, Technical Report, Sandia National Laboratories
Sridharan S, Zhu J, Hu G, Xuan X (2011) Joule heating effects on electroosmotic flow in insulator-based dielectrophoresis. Electrophoresis 32 (in press). doi:10.1002/elps.201100011
Srivastava SK, Gencoglu A, Minerick AR (2010) DC insulator dielectrophoretic applications in microdevice technology: a review. Anal Bioanal Chem 399:301–321
Srivastava SK, Baylon-Cardiel JL, Lapizco-Encinas BH, Minerick AR (2011) A continuous DC-insulator dielectrophoretic sorter of microparticles. J Chromatogr A 1218:1780–1789
Takagi J, Yamada M, Yasuda M, Seki M (2005) Continuous particle separation in a microchannel having asymmetrically arranged multiple branches. Lab Chip 5:778–784
Tsutsui H, Ho CM (2009) Cell separation by non-inertial force fields in microfluidic systems. Mech Res Commun 36:92–103
Vahey MD, Voldman J (2008) A new equilibrium method for continuous-flowcell sorting using dielectrophoresis. Anal Chem 80:3135–3143
Voldman J (2006) Electrical forces for microscale cell manipulation. Annu Rev Biomed Eng 8:425–454
Wang L, Lu J, Marchenko SA, Monuki ES et al (2009) Dual frequency dielectrophoresis with interdigitated sidewall electrodes for microfluidic flow-through separation of beads and cells. Electrophoresis 30:782–791
Wu ZG, Willing B, Bjerketorp J, Jansson JK, Hjort K (2009) Soft inertial microfluidics for high throughput separation of bacteria from human blood cells. Lab Chip 9:1193–1199
Xuan X (2008) Joule heating in electrokinetic flow. Electrophoresis 29:33–43
Xuan X, Zhu J, Church C (2010) Particle focusing in microfluidic devices. Microfluid Nanofluid 9:1–16
Yamada M, Seki M (2005) Hydrodynamic filtration for on-chip particle concentration and classification utilizing microfluidics. Lab Chip 5:1233–1239
Yamada M, Nakashima M, Seki M (2004) Pinched flow fractionation: continuous size separation of particles utilizing a laminar flow profile in a pinched microchannel. Anal Chem 76:5465–5471
Zhang CX, Manz A (2003) High-speed free-flow electrophoresis on chip. Anal Chem 75:5759–5766

Zhang C, Khoshmanesh K, Tovar-Lopez FJ, Mitchell A, Wlodarski W, Kalantar-Zadeh K (2009) Dielectrophoretic separation of carbon nanotubes and polystyrene microparticles. Microfluid Nanofluid 7:633–645

Zhu J, Xuan X (2009a) Dielectrophoretic focusing of particles in a microchannel constriction using DC-biased AC electric fields. Electrophoresis 30:2668–2675

Zhu J, Xuan X (2009b) Particle electrophoresis and dielectrophoresis in curved microchannels. J Colloid Interface Sci 340:285–290

Zhu J, Tzeng TJ, Hu G, Xuan X (2009) Dielectrophoretic focusing of particles in a serpentine microchannel. Microfluid Nanofluid 7:751–756

Zhu J, Tzeng TJ, Xuan X (2010a) Continuous dielectrophoretic separation of particles in a spiral microchannel. Electrophoresis 31:1382–1388

Zhu T, Marrero F, Mao L (2010b) Continuous separation of non-magnetic particles inside ferrofluids. Microfluid Nanofluid 9:1003–1009